The effect of catalyst preparation on the performance of magnesium fluoride supported ruthenium

Maria Wojciechowska [a,*], Mariusz Pietrowski [a], Sławomir Łomnicki [a,c] and Bogdan Czajka [b]

[a] *A. Mickiewicz University, Faculty of Chemistry, Poznań, Poland*
[b] *Central Laboratory of the Batteries and Cells, Poznań, Poland*
[c] *Foundation for Polish Science Stypendist*

Received 18 January 1997; accepted 4 April 1997

The effect of different ruthenium precursors on the structure and catalytic properties of the Ru/MgF_2 system was studied with such methods as IR, XPS, EPR and catalytic test reactions. The adsorption of probe molecules (CO and O_2) revealed a greater ability to transfer an electron from ruthenium in the case of samples obtained from $Ru_3(CO)_{12}$ than in the case of samples obtained from $RuCl_3$. Besides, metallic crystallites of different size were obtained depending on the precursor used. Namely, the average cluster size was 1.5 times smaller for carbonyl samples in comparison with chloride ones. Both series of preparations were active in redox or acid–base reactions. The activities of the carbonyl samples were higher than those of the chloride catalysts, particularly in reactions that require the presence of acid centers.

Keywords: ruthenium catalyst, Ru/MgF_2, precursor effect, IR, EPR, XRD

1. Introduction

Catalysts based on the noble metals have been used in many catalytic processes [1–6]. The discovery of metal–support interaction explains its great influence on the catalytic properties of such systems. This phenomenon is caused by modification of the metal electronic structure state due to charge transfer between the metal and the support [7,8]. In particular, ruthenium distinguishes itself among the group VIII metals. It is more active than platinum or rhodium [7]. Ruthenium is very active in reactions as hydrogenolysis of paraffins and olefins, Fischer–Tropsch synthesis and synthesis of oxygen containing compounds [9–16]. Literature provides works concerning ruthenium deposited on various supports, i.e., SiO_2 [7,18], Al_2O_3 [19,22], TiO_2 [21,22], and active carbon [23]. Such systems were synthesized using $RuCl_3$, $Ru_3(CO)_{12}$, $RuNO(NO_3)_3$, Ru(acac) or $Ru(NO_3)_3$ as the active phase precursor [8,17,19,24]. Great influence of the type of precursor and the methods of preparation and activation on the properties of ruthenium catalysts has been reported.

In this work the effect of the precursor on the properties of ruthenium supported on magnesium fluoride is discussed. The use of MgF_2 as a support for noble metal catalysts has not been studied so far, though it was found to have interesting properties as a transition metal oxide support.

2. Experimental

2.1. Preparation of catalysts

The Ru/MgF_2 samples were obtained by introduction of previously calcined (at 673 K, 4 h) MgF_2 with 0.25–0.50 grain size into an *n*-hexane solution of $Ru_3(CO)_{12}$ or aqueous solution of $RuCl_3$ for carbonyl and chloride samples, respectively. The suspension was evaporated, dried at 343 K for 24 h and next reduced under hydrogen flow at 673 K for 3 h.

The solutions taken for impregnation contained the appropriate amounts of ruthenium precursor to obtain samples containing 0.25, 0.50, 1.0 and 1.5 mol% ruthenium. The catalysts were hereafter denoted with the symbols CO-Ru_x and Cl-Ru_x depending on the precursor used, where x describes the ruthenium content in mol%.

2.2. Infrared spectra

IR spectra were recorded with a Bruker IFS 113V spectrometer in the range of the stretching vibrations of OH groups as well as the stretching and deformation vibrations of adsorbed pyridine. The experimental procedure was similar to that described in ref. [11].

For the IR study of CO adsorption the samples were placed in the form of thin wafers in an IR cell. Then the catalysts were reduced under hydrogen atmosphere for 1 h at 623 K, evacuated under vacuum for 1 h at 523 K and finally CO was admitted for 0.5 h at room tempera-

---

[*] To whom correspondence should be addressed.

© J.C. Baltzer AG, Science Publishers

ture, for 2 h and 4 h at 373 K. Then the CO was removed by evacuation at room temperature during 30 s and the spectra were recorded.

2.3. EPR spectra

The EPR spectra were taken at the temperature of liquid nitrogen (77 K) and at room temperature in the X-band on a Radiopan SE/X-2542 spectrometer.

2.4. XRD experiments

Diffractometric studies were performed with a Philips PW 1710 diffractometer using Cu Kα radiation, in the range of 5–152 2θ and in the low-angle range 0.1–52 2θ using a specific holder.

2.5. Catalytic experiments

The catalytic properties of the samples were determined by the pulse microreactor technique in the reactions of 2-propanol decomposition, dehydrogenation of cyclohexene, and isomerization of butene-1. The conditions of catalytic measurements were as follows:

2-propanol decomposition: reaction temperature 573 K, catalyst weight 0.01 g, volume size 0.2 μl, carrier gas flow (He) 30 cm^3/min, GC column 1 m Emulphor 0 at 60°C;

isomerization of butene-1: reaction temperature 573 K, catalyst weight 0.1 g, volume size 0.5 ml, carrier gas flow (He) 30 cm^3/min, GC column 10 m propylene carbonate at 0°C;

dehydrogenation of cyclohexene: reaction temperature 643 K, catalyst weight 0.1 g, volume size 0.2 μl, car-

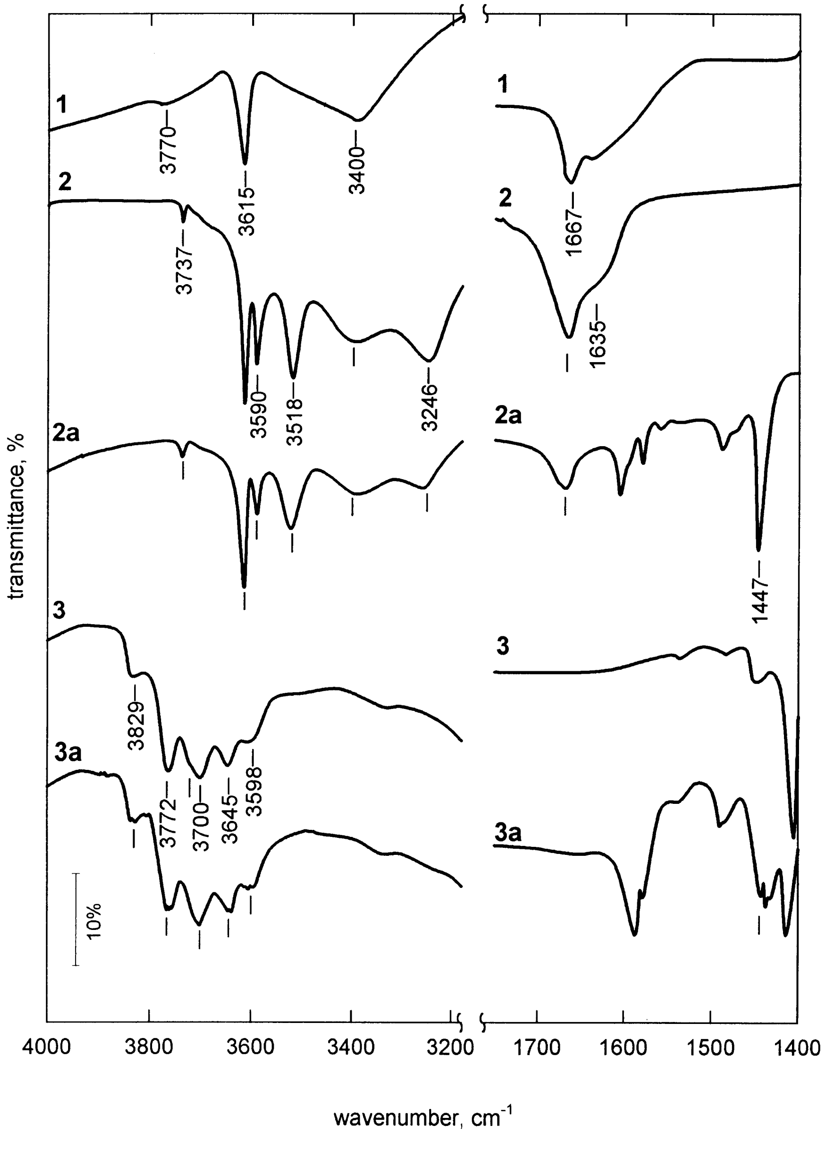

Figure 1. IR spectra of MgF_2 (curve 1), CO-$Ru_{1.0}$ (curves 2 and 2a) and Cl-$Ru_{1.0}$ (curves 3 and 3a).

rier gas flow (He) 20 cm^3/min, GC column 2 m propylene carbonate at room temperature.

Measurements of the catalytic activity in the hydrogenation reaction of nitrobenzene to aniline were performed by the flow method at 673 K. The mixture of nitrobenzene and hydrogen was passed through the microreactor at a volume rate of reactants introduction of 0.24 cm^3/h. The microreactor was filled with 0.25 g of catalyst. The products of the reaction were collected in the receiver at 273 K and analyzed by GC using a column filled with Apiezon L.

3. Results

3.1. IR results

Figure 1 presents the IR spectra of the series of CO-Ru and Cl-Ru preparations. In the spectrum of the CO-Ru preparation after deposition of ruthenium new bands were recorded at 3518, 3590, 3737 and 3246 cm^{-1} as well as bands originating from the OH group vibrations of magnesium fluoride at ~3400, 3615 cm^{-1} [25] and molecularly adsorbed water at ~1667 and 1635 cm^{-1} (spectrum 2, figure 1), which were not present in the spectrum of magnesium fluoride. The IR spectrum of the Cl-Ru sample shows the presence of a series intensive bands in the range of 3598–3829 cm^{-1} (3598, 3645, 3717, 3772, and 3829 cm^{-1}). However, the bands assigned to adsorbed molecular water were not detected in this case.

After introduction of pyridine vapors into both systems the bands corresponding to pyridine coordinatively bound to the surface of the samples were detected (spectra 2a and 3a, figure 1).

Adsorption of carbon monoxide at room temperature resulted in the appearance of bands at ~2000 (LF), 2095 (MF) and 2161 cm^{-1} (HF) in the spectrum of CO-Ru samples and ~2000, 2075 and 2140 cm^{-1} in that of the Cl-Ru ones (figure 2, the spectrum for CO-$Ru_{1.0}$ is presented as an example). The band at 2000 cm^{-1} originates from CO linearly adsorbed on metallic ruthenium, while the two other bands are assigned to CO adsorbed on partly oxidized $Ru^{\sigma+}$ species [21,29]. The intensity of all bands developed with increasing adsorption time.

3.2. EPR study

The signal characteristic of paramagnetic ruthenium species was not detected in the EPR spectra of both series of samples. Adsorption of probe molecules (O_2 and CO) resulted in the appearance of radical lines only in the spectra of the CO-Ru samples. Figure 3 presents the EPR spectrum of the latter after adsorption of CO. In this case a very intensive single line was recorded, with $g_0 = 2.002$ and 0.7 mT wide. This line is characteristic of a radical bound Ru-CO [30]. Similarly, after adsorption of O_2, on the broad line $\Delta B_{pp} = 120$ mT centered at $g_0 = 2.467$ in the field range 330–340 mT a weak radical spectrum characterized by $g_p = 2.017$ and $g_\perp = 2.001$ was observed. This spectrum corresponds to the O_2^- radical.

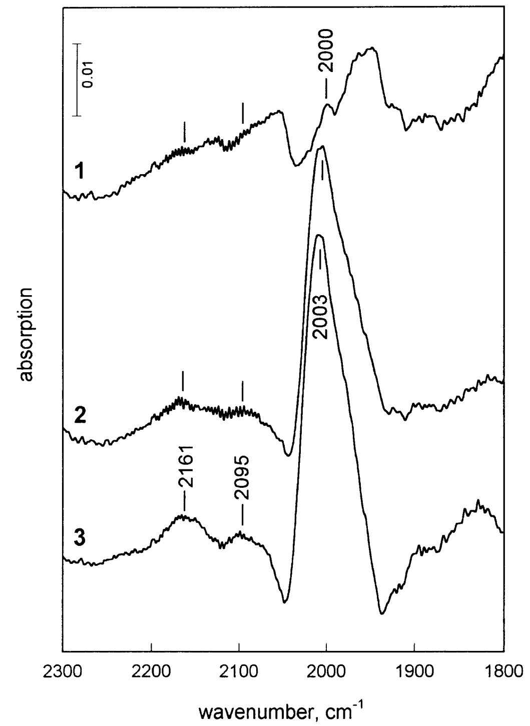

Figure 2. IR spectra of CO-$Ru_{1.0}$ after adsorption of CO for 0.5 h at room temperature (curve 1), 2 h at 373 K (curve 2), 4 h at 373 K (curve 3).

3.3. X-ray study

The X-ray study of the magnesium fluoride pretreated in the same way as the Ru/MgF_2 catalysts revealed only the lines characteristic for MgF_2 and Ru [31,32]. A Fourier analysis of the diffraction line of carbonyl sam-

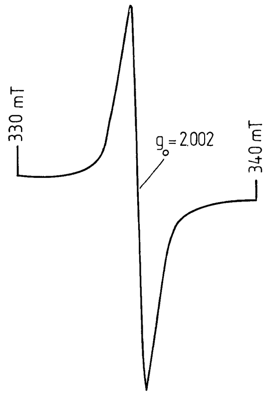

Figure 3. EPR spectrum at room temperature of the CO-$Ru_{1.0}$ sample reduced at 673 K in H_2 atmosphere after adsorption of CO.

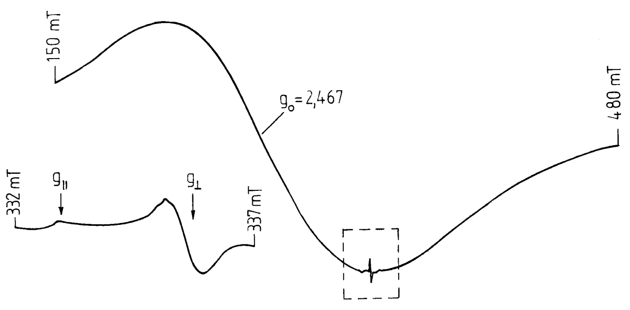

Figure 4. EPR spectrum at room temperature of the CO-$Ru_{1.0}$ sample reduced at 673 K in H_2 atmosphere after adsorption of O_2.

ples originating from MgF_2 $d = 1.63$ (*hkl* 220; I/I_0 30%) composed of 68 measure points in comparison with the same line of the pure support was made. In every case the same shape of the line was obtained with half-width 0.490 2θ. This indicates the absence of any disturbances of the lattice, also at the near surface layer.

The phase composition analysis of mechanically mixed magnesium fluoride and metallic ruthenium revealed that almost all lines of ruthenium and the support overlap. The only line not overlapped by the spectrum of the support was at $d = 0.867$. In the study of the sample containing the highest amount of ruthenium, i.e. 1.5 mol%, the presence of the third phase was not detected, however, the two near lines (covering each other) at $d = 1.232$ and $d = 1.208$ originating from MgF_2 and Ru, respectively, were separated.

The relative intensities of the above mentioned ruthenium diffraction lines were much higher for carbonyl samples than for the chloride ones. This suggests that the surface of Cl-Ru samples was more uniformly covered with metal than the surface of CO-Ru catalysts. In the latter system ruthenium forms bigger agglomerates of metal clusters.

Table 1 gives the relative intensities of diffraction lines as well as the crystallite sizes of the ruthenium. The sizes of crystallites in the carbonyl catalysts were much smaller relative to those of the chloride samples. Considerable differences in intensities of reflects of various series of samples suggest non-uniform covering of the surface or the presence of not high slices of metal on the surface of magnesium fluoride.

3.4. Catalytic activity

Figures 5–8 show the activities of the CO-Ru and Cl-Ru samples in various catalytic test reactions. In the 2-propanol decomposition to acetone and propene the samples obtained from $Ru_3(CO)_{12}$ were found to be more active than those obtained from $RuCl_3$ (figure 5), similarly to the case of the butene-1 isomerization reaction (figure 6). For these reactions the maximum activity of carbonyl samples was observed in the range of 0.5–1.0 mol% ruthenium loading. However, the activity of the chloride samples increased with the enrichment of the surface loading with Ru.

In the case of the cyclohexene dehydrogenation to benzene the highest activity of either carbonyl or chloride samples was similar, and the activity developed with increasing ruthenium loading (figure 7).

Both series of samples demonstrated high activity in the nitrobenzene hydrogenation to aniline (figure 8). However, the chloride samples with low ruthenium coverage (0.25 and 0.5 mol%) deactivated fast, whereas the carbonyl sample with 0.5 mol% of ruthenium was very active even after 6 h of reaction.

4. Discussion

Supported ruthenium is known to coordinate OH groups or water molecules [7]. In our IR investigations we also observed the bands originating from OH groups adsorbed on supported ruthenium. However, the IR results have shown considerable differences in hydroxyl layers of the CO-Ru and Cl-Ru samples. Namely, for the chloride samples the number of OH bands was almost three times greater than for the carbonyl ones. The authors of ref. [33] ascertained the presence of chloride ions in the Ru/γ-Al_2O_3 system when $RuCl_3$ was used as an active phase precursor, even after reduction of the sample with H_2. This indicates the incomplete reduction

Table 1
The average ruthenium crystallites sizes and relative reflects intensities ($d = 1.208$ and $d = 0.867$) for Ru/MgF_2 catalysts

Ru content (mol%)	Chloride series [a]			Carbonyl series		
	sample symbol	average cluster size (Å)	reflects intensities (arbitrary units)	sample symbol	average cluster size (Å)	reflects intensities (arbitrary units)
0.25	Cl-$Ru_{0.25}$	n.d.	n.d.	CO-$Ru_{0.25}$	155	106 91
0.50	Cl-$Ru_{0.50}$	235	13 24	CO-$Ru_{0.50}$	132	174 157
1.00	Cl-$Ru_{1.0}$	245	17 10	CO-$Ru_{1.0}$	137	48 34
1.50	Cl-$Ru_{1.5}$	265	18 19	CO-$Ru_{1.5}$	154	193 94

[a] n.d. = not detected.

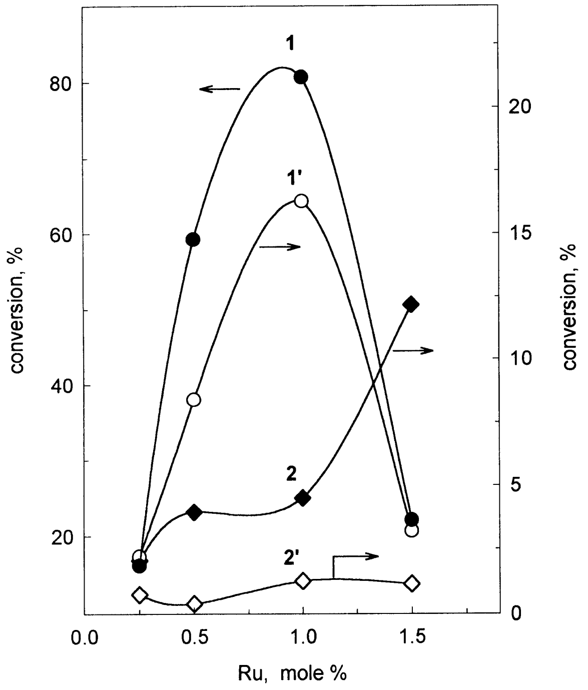

Figure 5. Catalytic behavior of carbonyl (1, 1′) and chloride (2, 2′) series of preparations in the decomposition of 2-propanol as a function of ruthenium content: 1 and 2 towards propene; 1′ and 2′ towards acetone.

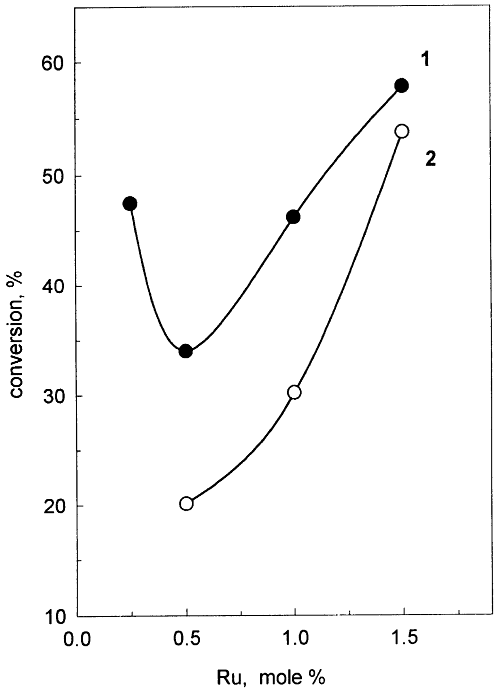

Figure 7. Catalytic behavior of carbonyl (1) and chloride (2) series of preparations in the dehydrogenation of cyclohexene as a function of ruthenium content.

of Ru^{3+} to Ru^0. One can expect a similar situation in the case of Ru/MgF_2 samples. Various oxidation states of ruthenium in Cl-Ru samples can explain the higher number of OH group bands when compared to those in the spectra of CO-Ru catalysts. One should note that ruthenium is known to coordinate hydroxyl groups easily [7].

The differences in the oxidation state of ruthenium

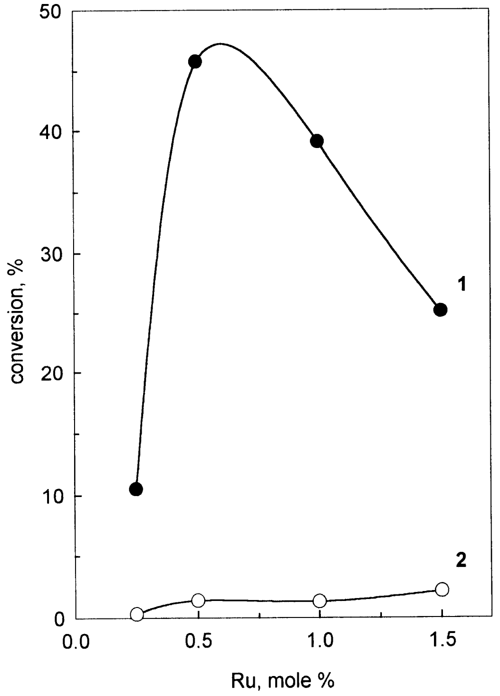

Figure 6. Catalytic behavior of carbonyl (1) and chloride (2) series of preparations in the isomerization of 1-butene as a function of ruthenium content.

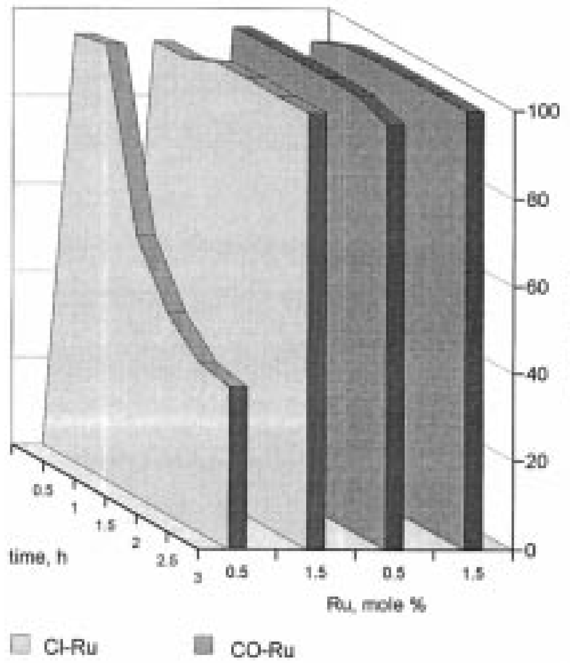

Figure 8. Catalytic behavior of carbonyl and chloride series of preparations in the hydrogenation of nitrobenzene to aniline as a function of ruthenium content.

obtained from various precursors were confirmed by EPR results. The appearance of the radical lines originating from O_2^- and CO^- in the spectra of the CO-Ru samples indicated the presence of ruthenium centers able to transfer an electron. Such an interaction with the probe molecules can proceed as follows:

$$Ru + CO \rightarrow Ru^+{-}CO^-$$

$$Ru + O_2 \rightarrow Ru^+{-}O_2^-$$

On the other hand, the lack of radical lines in the spectra of the Cl-Ru samples suggests that electron transfer was less probable due to the presence of Ru^{3+} and chloride ions.

The IR results of CO adsorption indicate the presence of Ru^0 in both series of preparations (LF band). Moreover, the appearance of the MF and HF bands corresponds to CO adsorbed on partially oxidized $Ru^{\sigma+}$ with an electric charge between 0 and 1. Similarly, the authors of refs. [21,29] assigned the LF bands to CO linearly adsorbed on the metallic crystallites of ruthenium in the Ru/Al_2O_3 system. However, they reported that the MF and HF bands are due to the dicarbonyl $Ru(CO)_2$ species, with Ru electric charge between 0 and 1. The difference in the position of the bands of adsorbed CO in the spectra of CO-Ru and Cl-Ru samples was a consequence of the ensemble size. Namely, Crisafulli et al. [34] found, that the smaller the crystallites of ruthenium, the higher the frequencies of the bands of adsorbed CO. Thus, the conclusion can be drawn that on the carbonyl preparations ruthenium is more dispersed than on the chloride samples. This conclusion was confirmed by the XRD experiments, which show that the average size of ruthenium clusters on CO-Ru samples is in the range 130–160 Å, while in chloride catalysts it varies from 230 to 270 Å. Considerable differences in the relative intensities of reflects of each series indicate uniform coverage of the surface with ruthenium clusters in the chloride samples and the growth of ruthenium clusters perpendicular to the surface in the carbonyl samples. The different distribution of ruthenium in these two types of catalysts can be assigned to the stabilizing effect of chloride anions. Namely, they hinder the reduction of ruthenium ions during hydrogen treatment and redistribution of ruthenium over the surface of the support. On the other hand, the migration of ruthenium clusters over the surface is not hindered during pretreatment for the carbonyl samples which results in multilayered clusters.

$Ru^{\sigma+}$ species can play the role of Lewis acid sites. The IR experiments of adsorption of pyridine revealed the existence of such centers. The band characteristic of pyridine bound to Lewis acid sites was detected at 1447 cm^{-1}. On the other hand no band characteristic of pyridinium ion was recorded, which indicated the lack of Brønsted acid sites. The catalytic test performed on both series of preparations confirmed the presence of acid centers. High activity of CO-Ru samples in the isomerization reaction of butene-1 indicated the presence of acid sites of medium strength, while Cl-Ru catalysts showed only little activity which meant that only few such centers were on their surface. These centers were not strong enough to compete with the surface redox sites. In the decomposition reactions of propanol-2 that can proceed – (a) dehydrogenation to acetone (redox sites) and (b) dehydration to propene (even weak acid sites) – the catalysts were mainly active in dehydrogenation.

Table 2
Catalytic activity of Ru/MgF_2 samples in nitrobenzene dehydrogenation to aniline expressed as TOF

Reaction time (h)	TOF			
	$Cl\text{-}Ru_{0.5}$	$Cl\text{-}Ru_{1.5}$	$CO\text{-}Ru_{0.5}$	$CO\text{-}Ru_{1.5}$
0.5	0.0319	0.0105	0.0325	0.0105
1.0	0.0275	0.0109	0.0325	0.0108
1.5	0.0195	0.0108	0.0325	0.0109
2.0	0.0150	0.0109	0.0325	0.0109
2.5	0.0126	0.0108	0.0324	0.0109
3.0	0.0120	0.0109	0.0316	0.0109

The activity of both series of Ru/MgF_2 samples in the dehydrogenation of cyclohexene and nitrobenzene hydrogenation to aniline also indicated the presence of a large number of redox sites on their surface. In particular in the latter reaction ruthenium catalysts were found to have almost 100% activity, and, moreover, the carbonyl samples remained active for a very long period. In table 2 TOF values for the nitrobenzene hydrogenation to aniline are presented. These data indicate, that the optimal composition of catalyst is 0.5 mol% of ruthenium.

Different precursors of ruthenium modify to a high degree the catalytic properties of the Ru/MgF_2 catalytic system affecting the oxidation state of Ru, which results in different acid–base and redox properties of the samples.

5. Conclusions

(1) Ru^0 as well as the $Ru^{\sigma+}$ species with charge between 0 and 1 occur in both chloride and carbonyl samples.

(2) Depending on the precursor used ruthenium clusters of different size are formed on the surface of the support. $Ru_3(CO)_{12}$ promotes the formation of smaller crystallites than ruthenium chloride.

(3) The surface ruthenium of the carbonyl catalysts interact with π^*-acceptor molecules, that is ruthenium deposited on magnesium fluoride is capable of donating an electron to the adsorbed molecules.

(4) The Ru/MgF_2 systems are active in reactions that require the presence of redox and acidic centers.

(5) The carbonyl catalysts are more active than the chloride catalysts in acidic reactions.

References

[1] U. Kiiski, T.A. Pakkanen and O. Krause, J. Mol. Catal. 50 (1989) 143.
[2] Y. Doi, A. Yokota, H. Miyake and K. Soga, J. Chem. Soc. Chem. Commun. (1984) 394.
[3] Y. Doi, K. Soga, K. Yano and Y. Ono, J. Mol. Catal. 19 (1983) 358.
[4] Y. Doi, K. Yano, A. Yokota, H. Miyake and K. Soga, *8th Int. Congr. on Catalysis*, Berlin 1984, IV-689.
[5] J. Lieto, J.J. Rafalko and B.C. Gates, J. Catal. 62 (1980) 149.
[6] Z. Otero-Schipper, J. Lieto and B.C. Gates, J. Catal. 63 (1980) 175.
[7] T. Lopez, P. Bosch, M. Asomoza and R. Gomez, J. Catal. 133 (1992) 247.
[8] L. Yongxue, W. Shuguang and X. Qin, React. Kinet. Catal. Lett. 38 (1989) 63.
[9] J.H. Sinfelt, Catal. Rev. 3 (1969) 175.
[10] J.H. Sinfelt and D.J.C. Yates, J. Catal. 8 (1967) 82.
[11] J.C. Kempling and R.B. Anderson, Ind. Eng. Chem. Process Des. Dev. 9 (1970) 116; 11 (1967) 146.
[12] V. Ragaini, L. Forni and R. Le Van Mao, J. Catal. 37 (1975) 339.
[13] V. Ragaini, A. Spadaro and G. Cum, React. Kinet. Catal. 2 (1975) 19, 135.
[14] M.A. Vannice, in: *Catalysis Science and Technology*, Vol. 3, eds. J.R. Anderson and M. Boudart (Springer, Berlin, 1981) ch. 3, pp. 154, 179.
[15] M.E. Dry, in: *Catalysis Science and Technology*, Vol. 1, eds. J.R. Anderson and M. Boudart (Springer, Berlin, 1981) ch. 4, p. 194.
[16] R.C. Everson, E.T. Woodburn and A.R. Kirk, J. Catal. 53 (1978) 186.
[17] E. Rodriguez, M. Leconte, J.M. Basset and K. Tanaka, J. Catal. 119 (1989) 230.
[18] E. Rodriguez, M. Leconte and J.M. Basset, J. Catal. 131 (1991) 457.
[19] J.A. Mieth and J.A. Schwartz, J. Catal. 118 (1989) 203.
[20] M.G. Cattania Sabbadini, A. Gervasini, F. Morazzoni and D. Strumulo, J. Chem. Soc. Faraday Trans. I 83 (1987) 2271.
[21] N.M. Gupta, V.S. Kamble, R.M. Iyer, K.R. Thampi and M. Grätzel, J. Catal. 137 (1992) 473.
[22] M. Grätzel, K.R. Thampi, J. Kiwi and J.G. Highfield, in: *Proc. 2nd European Conf. on Catalysis*, eds. G.M. Schwab, Berlin-Spandau-Johannesstift 1989, p. 42
[23] C. Moreno-Castilla, M.A. Salas-Peregrín and F.J. López-Garzón, J. Mol. Catal. 95 (1995) 223.
[24] B. Coq, A. Bittar and F. Figueras, Appl. Catal. 59 (1990) 103.
[25] J. Haber and M. Wojciechowska, J. Catal. 110 (1988) 23.
[26] J. Haber, J. Stoch and M. Wojciechowska, Surf. Interf. Anal. 15 (1990) 711.
[27] J. Haber and M. Wojciechowska, in: *Science and Technology in Catalysis 1994*, Stud. Surf. Sci. Catal., Vol. 92, eds. Y. Izumi, H. Arai and M. Iwamoto (Elsevier/Kodansha, Amsterdam/Tokyo, 1995) p. 87.
[28] M. Wojciechowska, S. Łomnicki, J. Bartoszewicz and J. Goslar, J. Chem. Soc. Faraday Trans. 91 (1995) 2207.
[29] F. Solymosi and J. Raskó, J. Catal. 115 (1989) 107.
[30] M. Haga, E.S. Dodsworth and A.B.P. Lever, Inorg. Chem. 25 (1986) 447.
[31] NBS Circular 539, Vol. IV (1955) p. 33.
[32] NBS Circular 539, Vol. IV (1955) p. 5.
[33] A. Bossi, F. Garbassi, G. Petrini and L. Zanderighi, J. Chem. Soc. Faraday Trans. I 78 (1982) 1029.
[34] C. Crisafulli, R. Maggiore, S. Sciré, S. Galvagno and C. Milone, J. Mol. Catal. 83 (1993) 237.